IOPscience iopscience.iop.org

Home Search Collections Journals About Contact us My IOPscience

Multiple scattering in a vacuum barrier obtained from real-space wavefunctions

This article has been downloaded from IOPscience. Please scroll down to see the full text article.

2005 J. Phys.: Condens. Matter 17 2705

(http://iopscience.iop.org/0953-8984/17/17/019)

View the table of contents for this issue, or go to the journal homepage for more

Download details:
IP Address: 129.252.86.83
The article was downloaded on 27/05/2010 at 20:41

Please note that terms and conditions apply.

INSTITUTE OF PHYSICS PUBLISHING JOURNAL OF PHYSICS: CONDENSED MATTER

J. Phys.: Condens. Matter **17** (2005) 2705–2713 doi:10.1088/0953-8984/17/17/019

Multiple scattering in a vacuum barrier obtained from real-space wavefunctions

Krisztián Palotás[1] **and Werner A Hofer**[1,2,3]

[1] Surface Science Research Centre and Department of Physics, University of Liverpool, Liverpool L69 3BX, UK
[2] Donostia International Physics Centre, San Sebastian, Spain

E-mail: whofer@liverpool.ac.uk

Received 4 February 2005, in final form 22 March 2005
Published 15 April 2005
Online at stacks.iop.org/JPhysCM/17/2705

Abstract

We have developed a method for simulating multiple electron scattering in a vacuum barrier using real-space single-electron wavefunctions for the separate surfaces. The Green functions in the vacuum barriers are calculated to first order in the Dyson series. We find that the zero-order current is equal to the usual Bardeen approach only in the limit of zero bias and derive the modifications in the finite bias regime. We also derive a first-principles formulation for the energy of interaction between the two surfaces, and show that it is proportional to the tunnelling current. With this method the tunnelling current can in principle be computed to any order in the Dyson expansion.

(Some figures in this article are in colour only in the electronic version)

1. The Keldysh formalism in a vacuum barrier

From a theoretical point of view a tunnelling electron, e.g. in a scanning tunnelling microscopy measurement, is part of a system comprising two infinite metal leads and an interface, consisting of a vacuum barrier and, optionally, a molecule or a cluster of atoms with different properties to the infinite leads. The system can be said to be open—the number of charge carriers is not constant—and out of equilibrium—the applied potential and the charge transport itself introduce polarizations and excitations within the system. The theoretical description of such a system has advanced significantly over the last few years; to date the most comprehensive description is based either on a self-consistent solution of the Lippman–Schwinger equation [1] or on the non-equilibrium Green function approach [2–6]. Within the non-equilibrium formalism the current through a conductor from lead A to lead B is described by [3]

$$I = \frac{e}{h}\int_{\mu_A - eV}^{\mu_B + eV} \mathrm{d}E\ \mathrm{Tr}\left[\Sigma_A^<(E)G^>(E) - \Sigma_A^>(E)G^<(E)\right]. \tag{1}$$

[3] Author to whom any correspondence should be addressed.

 © 2005 IOP Publishing Ltd Printed in the UK

Inelastic effects within e.g. a molecule–surface interface can be included by considering multiple electron paths from the vacuum into the surface substrate [7]. Within the vacuum barrier itself, inelastic effects play an insignificant role. Here, as in most experiments in scanning tunnelling microscopy, the problem can be reduced to the description of the tunnelling current between two leads—the surface S and the tip T—thought to be in thermal equilibrium. The bias potential of the circuit is in this case described by a modification of the chemical potentials of surface and tip system, symbolized by μ_S and μ_T. This reduces the tunnelling problem to the Landauer–Büttiker formulation [3, 8], or

$$I = \frac{2e}{h}\int_{-\infty}^{+\infty} \mathrm{d}E\,[f(\mu_S, E) - f(\mu_T, E)]\,\mathrm{Tr}\left[\Gamma_T(E)G^R(E)\Gamma_S(E)G^A(E)\right]. \tag{2}$$

Here, f denotes the Fermi distribution function, $G^{R\,(A)}(E)$ is the retarded (advanced) Green function of the barrier, and Γ_S, Γ_T are the surface and tip contacts, respectively. They correspond to the difference of retarded and advanced self-energy terms of the surface and tip; we define them by their relation to the spectral function $A_{S\,(T)}$ of the surface (tip) [3]:

$$A_{S\,(T)} = i\left[G^R_{S\,(T)} - G^A_{S\,(T)}\right] = G^R_{S\,(T)}\Gamma_{S\,(T)}G^A_{S\,(T)}. \tag{3}$$

Here, the explicit energy dependence has been omitted for brevity. At present, these equations are evaluated within localized basis sets, and in a matrix representation. From a theoretical point of view this requires one to either represent the electronic properties of the two surfaces also in a localized representation [5, 6], or to transform the plane wave basis set of most density functional methods to a local basis. The use of local basis sets compromises the numerical accuracy in the tunnelling barrier, since the vacuum tails of the surface wavefunctions decay too rapidly: the constant current contours in this case are too close to the surface.

2. Calculating the current from real-space wavefunctions

Here we present a formulation of the problem which is based on the Green functions of the two surfaces, given in a real-space representation based on the electronic eigenstates of the two systems. We show how the multiple-scattering formalism described in equation (2) can be evaluated in real space, and how it relates to the perturbation expansion of the tunnelling problem. We start with an eigenvector expansion of the surface and tip Green functions, given by

$$G_S^{R\,(A)}(\mathbf{r}_1, \mathbf{r}_2, E) = \sum_i \frac{\psi_i(\mathbf{r}_1)\psi_i^*(\mathbf{r}_2)}{E - E_i' + (-)\mathrm{i}\eta} \tag{4}$$

$$G_T^{R\,(A)}(\mathbf{r}_1, \mathbf{r}_2, E) = \sum_j \frac{\chi_j(\mathbf{r}_1)\chi_j^*(\mathbf{r}_2)}{E - E_j' + (-)\mathrm{i}\epsilon}. \tag{5}$$

Throughout this paper the wavefunctions ψ and χ denote the Kohn–Sham states of surface and tip, respectively, resulting from a density functional calculation. The energy levels are shifted due to the applied bias voltage (see figure 1), so $E_i' = E_i - eV/2$, $E_j' = E_j + eV/2$. The set-up of the system is shown in figure 1(a). The spectral function A_S describes the charge density matrix; from equation (3) we find

$$A_S(\mathbf{r}_1, \mathbf{r}_2, E) = 2\eta\sum_i \frac{\psi_i(\mathbf{r}_1)\psi_i^*(\mathbf{r}_2)}{(E - E_i')^2 + \eta^2}. \tag{6}$$

The spectral function is related to Γ_S by equation (3). With the ansatz for Γ_S:

$$\Gamma_S(\mathbf{r}_3, \mathbf{r}_4, E) = C\sum_j \psi_j(\mathbf{r}_3)\psi_j^*(\mathbf{r}_4) \tag{7}$$

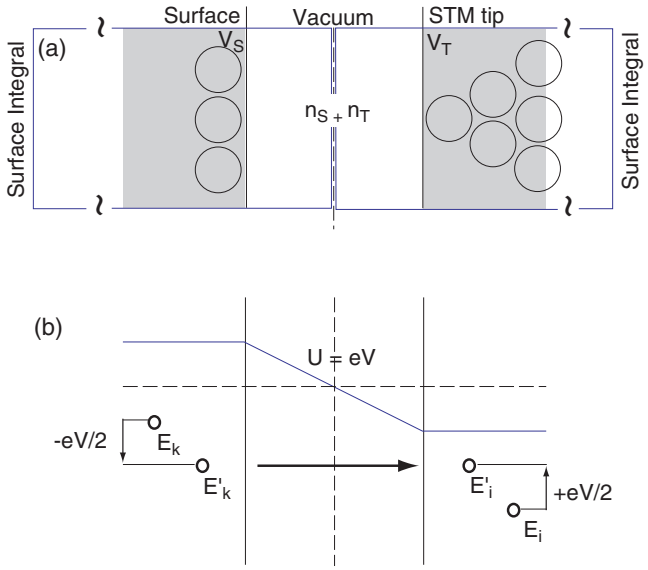

Figure 1. (a) The system under consideration, and the surface integrals used in deriving the zero-order current. (b) The effect of finite bias potentials: in this case the eigenvalues are shifted by $\pm eV/2$.

where C is a constant, we perform the double volume integration of equation (3). In this case the orthogonality of surface states reduces the expression to a compact form:

$$C\int \mathrm{d}^3r_3\,\mathrm{d}^3r_4\,G_{\mathrm{S}}^{\mathrm{R}}(\mathbf{r}_1,\mathbf{r}_3,E)\Gamma_{\mathrm{S}}(\mathbf{r}_3,\mathbf{r}_4,E)G_{\mathrm{S}}^{\mathrm{A}}(\mathbf{r}_4,\mathbf{r}_2,E)$$
$$= C\sum_{ijk}\frac{\psi_i(\mathbf{r}_1)\psi_k^*(\mathbf{r}_2)\delta_{ij}\delta_{jk}}{(E-E_i'+\mathrm{i}\eta)(E-E_k'-\mathrm{i}\eta)}. \tag{8}$$

Comparing the result with equation (6) we find for the contacts of surface and tip,

$$\Gamma_{\mathrm{S}} = 2\eta\sum_k \psi_k(\mathbf{r}_3)\psi_k^*(\mathbf{r}_4), \qquad \Gamma_{\mathrm{T}} = 2\epsilon\sum_i \chi_i(\mathbf{r}_1)\chi_i^*(\mathbf{r}_2). \tag{9}$$

For the construction of the Green function in the barrier we use the fact that the charge density is known from the separate calculation for the surface and tip. In the limit of weak coupling, the total charge density of the interface is given by (see figure 1)

$$n(\mathbf{r},E) = \sum_i \psi_i(\mathbf{r})\psi_i^*(\mathbf{r})\delta(E-E_i') + \sum_j \chi_j(\mathbf{r})\chi_j^*(\mathbf{r})\delta(E-E_j'). \tag{10}$$

This indicates that a zero-order approximation for the Green function of the vacuum barrier can be constructed as a sum of surface and tip Green functions, or

$$G_{(0)}^{\mathrm{R\,(A)}}(\mathbf{r}_1,\mathbf{r}_2,E) = G_{\mathrm{S}}^{\mathrm{R\,(A)}}(\mathbf{r}_1,\mathbf{r}_2,E) + G_{\mathrm{T}}^{\mathrm{R\,(A)}}(\mathbf{r}_1,\mathbf{r}_2,E). \tag{11}$$

The imaginary part of the diagonal elements $\mathbf{r}_1 = \mathbf{r}_2$ of this Green function is just equal to the total charge density. For the off-diagonal elements $\mathbf{r}_1 \neq \mathbf{r}_2$ we demonstrate using two separate estimates that this choice is justified. First, from the Schrödinger equation:

$$\left[-\frac{\hbar^2}{2m}\nabla^2 + V_{\mathrm{S}}(\mathbf{r}_1) + V_{\mathrm{T}}(\mathbf{r}_1)\right](G_{\mathrm{S}}(\mathbf{r}_1,\mathbf{r}_2) + G_{\mathrm{T}}(\mathbf{r}_1,\mathbf{r}_2)) = 0 \tag{12}$$

it follows that the Green function is exact if

$$V_{\mathrm{S}}(\mathbf{r}_1)G_{\mathrm{T}}(\mathbf{r}_1,\mathbf{r}_2)+V_{\mathrm{T}}(\mathbf{r}_1)G_{\mathrm{S}}(\mathbf{r}_1,\mathbf{r}_2)=0. \tag{13}$$

In the surface region $V_{\mathrm{T}}=0$ and $G_{\mathrm{T}}\approx 0$. In the tip region $V_{\mathrm{S}}=0$ and $G_{\mathrm{S}}\approx 0$. In the vacuum region both terms are products of functions centred on different sides of the vacuum barrier and decaying exponentially: they are consequently very small in comparison to other terms. Thus equation (13) approximately holds throughout the whole system. Second, let us write a well known property of the Green function:

$$\frac{\partial G(z)}{\partial z}=-G^2(z). \tag{14}$$

Substituting equation (11) into this formula results in the following condition: $G_{\mathrm{S}}(z)G_{\mathrm{T}}(z)=0$. This is approximately satisfied over the whole system because in the surface region $G_{\mathrm{T}}\approx 0$, in the tip region $G_{\mathrm{S}}\approx 0$, and in the vacuum region

$$G_{\mathrm{S}}G_{\mathrm{T}}\propto\frac{\mathrm{e}^{-\kappa_{\mathrm{S}}|\mathbf{r}-\mathbf{r}'|}}{|\mathbf{r}-\mathbf{r}'|}\frac{\mathrm{e}^{-\kappa_{\mathrm{T}}|\mathbf{r}-\mathbf{r}''|}}{|\mathbf{r}-\mathbf{r}''|}\approx 0. \tag{15}$$

Now all the necessary components for calculating the trace in the non-equilibrium formalism are given in terms of the real-space surface and tip wavefunctions. We obtain the following expression for the trace:

$$\begin{aligned}\mathrm{Tr}\left[\Gamma_{\mathrm{T}}G^{\mathrm{R}}_{(0)}\Gamma_{\mathrm{S}}G^{\mathrm{A}}_{(0)}\right]=\sum_{ik}|A_{ik}|^2\Bigg[&\frac{4\eta\epsilon}{(E-E'_k)^2+\eta^2}+\frac{4\eta\epsilon}{(E-E'_k+\mathrm{i}\eta)(E-E'_i-\mathrm{i}\epsilon)}\\&+\frac{4\eta\epsilon}{(E-E'_k-\mathrm{i}\eta)(E-E'_i+\mathrm{i}\epsilon)}+\frac{4\eta\epsilon}{(E-E'_i)^2+\epsilon^2}\Bigg]\end{aligned} \tag{16}$$

with the overlap integral A_{ik} given by

$$A_{ik}=\int \mathrm{d}^3r\;\chi_i^*(\mathbf{r})\psi_k(\mathbf{r}). \tag{17}$$

The sum of fractions involving energies and ϵ, η, which results from the multiplication of Green functions, can be written in a more compact way as

$$\frac{(E-E'_k+E-E'_i)^2+(\eta+\epsilon)^2}{[(E-E'_k)^2+\eta^2][(E-E'_i)^2+\epsilon^2]}. \tag{18}$$

In the limit $\eta,\epsilon\to+0$ the second term in the numerator will vanish, and since

$$\lim_{\eta\to 0}\frac{\eta}{(E-E'_i)^2+\eta^2}=\pi\delta(E-E'_i), \tag{19}$$

the transmission probability reduces to

$$\sum_{ik}|A_{ik}|^2 4\pi^2\delta(E-E'_k)\delta(E-E'_i)(E-E'_k+E-E'_i)^2. \tag{20}$$

The calculation of the matrix elements A_{ik} involves an integration over infinite space, which cannot be directly performed. To convert the volume integrals into surface integrals we use the fact that the vacuum states of the surface and tip are free electron solutions with characteristic decay constants, complying with the vacuum Schrödinger equation:

$$\frac{\hbar^2}{2m}(\nabla^2+\kappa_i^2)\chi_i(\mathbf{r})=0\Rightarrow\chi_i(\mathbf{r})=-\frac{\nabla^2}{\kappa_i^2}\chi_i(\mathbf{r}) \tag{21}$$

$$\frac{\hbar^2}{2m}(\nabla^2+\kappa_k^2)\psi_k(\mathbf{r})=0\Rightarrow\psi_k(\mathbf{r})=-\frac{\nabla^2}{\kappa_k^2}\psi_k(\mathbf{r}). \tag{22}$$

In addition we make use of the following identities:

$$\chi_i^* \nabla^2 \psi_k = \nabla(\chi_i^* \nabla \psi_k) - \nabla \chi_i^* \nabla \psi_k$$
$$\psi_k \nabla^2 \chi_i^* = \nabla(\psi_k \nabla \chi_i^*) - \nabla \chi_i^* \nabla \psi_k.$$

After some trivial manipulations, and making use of Gauss's theorem, this allows us to convert the volume integral into an integral over the separation surface (see figure 1):

$$A_{ik} = \frac{1}{\kappa_i^2 - \kappa_k^2} \int \mathrm{d}S \left[\chi_i^*(\mathbf{r}) \nabla \psi_k(\mathbf{r}) - \psi_k(\mathbf{r}) \nabla \chi_i^*(\mathbf{r}) \right] =: \frac{M_{ik}}{\kappa_i^2 - \kappa_k^2}. \tag{23}$$

It should be mentioned that the above expression only holds for $\kappa_i \neq \kappa_k$. In practice, this will not affect the general validity of the method, since STM measurements are done with different surface and tip materials, possessing a different spectrum of eigenvalues with different vacuum decay constants. But even if the decay constants are equal, the overlap integral will still be finite. This surface integral is well known; apart from the universal constant $\hbar^2/2m$ it describes the tunnelling matrix element in the perturbation approach [9, 10].

3. Zero-order current

Integrating over the energy range, we obtain from equations (2), (20), and (23) the tunnelling current in the zero-order approximation:

$$I_{(0)} = \frac{4\pi e}{\hbar} \sum_{ik} \left[f(\mu_\mathrm{S}, E_k') - f(\mu_\mathrm{T}, E_i') \right] \left| \frac{(E_k' - E_i') M_{ik}}{\kappa_i^2 - \kappa_k^2} \right|^2 \delta(E_i' - E_k'). \tag{24}$$

The decay constants are proportional to the eigenvalues shifted by the bias voltage of the tunnelling junction:

$$E_i = \frac{\hbar^2 \kappa_i^2}{2m} = E_i' - \frac{eV}{2}; \qquad E_k = \frac{\hbar^2 \kappa_k^2}{2m} = E_k' + \frac{eV}{2}. \tag{25}$$

Including the effect of finite bias voltages thus leads to the following result:

$$I_{(0)} = \frac{4\pi e}{\hbar} \sum_{ik} \left[f\left(\mu_\mathrm{S}, E_k - \frac{eV}{2}\right) - f\left(\mu_\mathrm{T}, E_i + \frac{eV}{2}\right) \right] \times \left| \left(-\frac{\hbar^2}{2m} - \frac{eV}{\kappa_i^2 - \kappa_k^2} \right) M_{ik} \right|^2 \delta(E_i - E_k + eV). \tag{26}$$

It can be seen from this formulation that the tunnelling spectrum obtained, or the $\mathrm{d}I/\mathrm{d}V$ curves, will increase quadratically with the applied bias voltage. This is actually observed in spectroscopy experiments [11]. We shall present a detailed calculation of tunnelling spectra and a comparison with experimental data further down. The second term in brackets, giving the bias dependence in the zero-order scattering approach, is a correction to the standard Bardeen approach, which can be recovered in the limit of zero bias. In this case we confirm the result given by Feuchtwang and Pendry *et al* [12, 13], that the Bardeen method is just the zero-order approximation, in the limit of zero bias, to a full scattering treatment [9, 10]:

$$I_\mathrm{B} = \frac{4\pi e}{\hbar} \sum_{ik} [f(\mu_\mathrm{S}, E_k) - f(\mu_\mathrm{T}, E_i)] \left| -\frac{\hbar^2}{2m} M_{ik} \right|^2 \delta(E_i - E_k). \tag{27}$$

This result and its interpretation in terms of scattering theory are well accepted. Here, it shows once more that the choice for the zero-order Green function of the interface is justified. It should be noted that the bias dependence will also affect the result of a derivation which is based on an analytical form of the tip wavefunctions, e.g. the Tersoff–Hamann approach [14].

There, the matrix element $|M_{ik}|^2$ is replaced by the charge density $|\psi_k(\mathbf{R})|^2$, where $\mathbf{R}$ is the centre of the STM tip apex. This means that the modified Tersoff–Hamann result, including the bias dependence, will be the following:

$$I_{\mathrm{TH}} \propto \left| \left(-\frac{\hbar^2}{2m} - \frac{eV}{\kappa_{\mathrm{T}}^2 - \kappa_k^2} \right) \psi_k \right|^2, \tag{28}$$

where κ_{T} is the decay length of the tip s orbital.

4. First-order Green function

The approach can be extended to higher orders. In the first-order expansion of the Dyson series the Green function is given by

$$G^{\mathrm{R}}_{(1)} = G^{\mathrm{R}}_{(0)} + G^{\mathrm{R}}_{(0)} V G^{\mathrm{R}}_{(0)}. \tag{29}$$

To calculate the first-order Green function for systems out of equilibrium, the equation has to be solved self-consistently [1, 5]. Self-consistency can in principle also be achieved by basing the calculation on the Kohn–Sham states ψ and χ of charged surfaces [16]. Under tunnelling conditions, however, the leads are in thermal equilibrium and the systems only weakly coupled. V in this case is the potential $V_{\mathrm{S}} + V_{\mathrm{T}}$ within the vacuum barrier:

$$G^{\mathrm{R}}_{(1)}(\mathbf{r}_1, \mathbf{r}_2) = G^{\mathrm{R}}_{(0)}(\mathbf{r}_1, \mathbf{r}_2) + \int \mathrm{d}r_3 \, G^{\mathrm{R}}_{(0)}(\mathbf{r}_1, \mathbf{r}_3) \left[V_{\mathrm{S}}(\mathbf{r}_3) + V_{\mathrm{T}}(\mathbf{r}_3) \right] G^{\mathrm{R}}_{(0)}(\mathbf{r}_3, \mathbf{r}_2). \tag{30}$$

This leads to six additional first-order terms, described by

$$G_{(1)} = G_{(0)} + G_{\mathrm{S}} V_{\mathrm{T}} G_{\mathrm{S}} + G_{\mathrm{T}} V_{\mathrm{S}} G_{\mathrm{T}} + G_{\mathrm{S}} V_{\mathrm{T}} G_{\mathrm{T}} + G_{\mathrm{S}} V_{\mathrm{S}} G_{\mathrm{T}} + G_{\mathrm{T}} V_{\mathrm{S}} G_{\mathrm{S}} + G_{\mathrm{T}} V_{\mathrm{T}} G_{\mathrm{S}}. \tag{31}$$

Here, the first line corresponds to excitations on either side of the tunnelling junction, the second line describes the effects due to transitions. In the following we focus on transitions; we note, however, that excitations can be included in the formulation by a suitable adaptation of many-body theory. Writing the first term of the second line explicitly, and with the shortcut $f^{\pm}_{ik} = (E - E'_i \pm \mathrm{i}\eta)(E - E'_k \pm \mathrm{i}\epsilon)$, we get

$$G^{\mathrm{R}}_{\mathrm{S}} V_{\mathrm{T}} G^{\mathrm{R}}_{\mathrm{T}} = \sum_{ik} \frac{\psi_i(\mathbf{r}_1) \chi^*_k(\mathbf{r}_2)}{f^+_{ik}} \int \mathrm{d}^3 r \, \psi^*_i(\mathbf{r}) V_{\mathrm{T}}(\mathbf{r}) \chi_k(\mathbf{r}). \tag{32}$$

Apart from an insignificant contribution in the surface region the integral is just the Bardeen matrix element in the zero-order expansion [10, 15], or the integral over the tip region Ω_{T}:

$$\int_{\Omega_{\mathrm{T}}} \mathrm{d}^3 r \, \psi^*_i(\mathbf{r}) V_{\mathrm{T}}(\mathbf{r}) \chi_k(\mathbf{r}) = -\frac{\hbar^2}{2m} M^*_{ki}. \tag{33}$$

Since the perturbative treatment is completely symmetric with respect to the surface and tip system, we find equally for the second term, by integration over the surface region Ω_{S},

$$\begin{aligned} G^{\mathrm{R}}_{\mathrm{S}} V_{\mathrm{S}} G^{\mathrm{R}}_{\mathrm{T}} &= \sum_{ik} \frac{\psi_i(\mathbf{r}_1) \chi^*_k(\mathbf{r}_2)}{f^+_{ik}} \int \mathrm{d}^3 r \, \psi^*_i(\mathbf{r}) V_{\mathrm{S}}(\mathbf{r}) \chi_k(\mathbf{r}) \\ &= -\frac{\hbar^2}{2m} \sum_{ik} \frac{\psi_i(\mathbf{r}_1) \chi^*_k(\mathbf{r}_2)}{f^+_{ik}} M^*_{ki}. \end{aligned} \tag{34}$$

The first-order Green function of the interface reads then

$$G^{\mathrm{R\,(A)}}_{(1)} = G^{\mathrm{R\,(A)}}_{(0)} - \frac{\hbar^2}{m} \sum_{ik} \frac{\psi_i(\mathbf{r}_1) M^*_{ki} \chi^*_k(\mathbf{r}_2) + \chi_k(\mathbf{r}_1) M_{ki} \psi^*_i(\mathbf{r}_2)}{f^{+(-)}_{ik}}. \tag{35}$$

It is evident that each subsequent iteration in the interface Green function can also be formulated in terms of Bardeen matrix elements: in principle, the Green function and thus the current can therefore be evaluated to any order.

5. Interaction energy

Finally, we calculate the energy of interaction between the surface and the tip in the low coupling limit. It has been shown recently by an analysis of first-order perturbation expressions for the tunnelling current and the interaction energy that the two variables should be linear with each other. From the first-order Green function we may construct the density matrix $\hat{n} = -\mathrm{i}/2\pi(G^{\mathrm{A}} - G^{\mathrm{R}})$. The interaction energy is then [17]

$$E_{\mathrm{int}} = -\frac{\mathrm{i}}{2\pi}\int_{-\infty}^{+\infty} \mathrm{d}E\ \mathrm{Tr}[(G^{\mathrm{A}}_{(1)}(E) - G^{\mathrm{R}}_{(1)}(E))(V_{\mathrm{S}} + V_{\mathrm{T}})]. \tag{36}$$

With $G^{\mathrm{R\,(A)}}_{(1)}$ from equation (35) this leads to

$$E_{\mathrm{int}} = -4\left(\frac{\hbar^2}{m}\right)^2 \sum_{ik} \frac{|M_{ki}|^2}{|E_i - E_k + eV|}. \tag{37}$$

The absolute value of the denominator is due to integrating the infinite energy interval in two steps, and taking each result separately as a contribution to the interaction energy. The calculation of the interaction energy only involves the computation of the tunnelling matrix elements. As shown previously, the interaction energy will therefore be proportional to the tunnelling current [17].

6. The spectrum of Fe(001)

The method has been applied to the calculation of the differential spectra of Fe(001), measured with a tungsten tip [18]. The system is well known and spectroscopic data are available in the literature (see e.g. [11]). The surface possesses a surface state near the $\bar{\Gamma}$ point, at an energy of +0.2 eV. We have made calculations for a 13-layer Fe(001) film with standard DFT methods [19, 20], using projector augmented waves for higher precision [21], and a generalized gradient approximation for the exchange–correlation potentials [22]. The two surface layers were fully relaxed. In the final iteration we used 465 k-points in the irreducible wedge of the Brillouin zone to obtain a dense map of the electronic structure. The STM tip model was calculated in a similar fashion; we used a 13-layer tungsten tip with an atomically sharp apex. The tip states were mapped with 100 k-points at the very centre of the Brillouin zone. The spectrum was calculated for a bias range from −2.5 to +2.5 V. As described in [18], the differential $\mathrm{d}I/\mathrm{d}V$ curve is directly obtained for every energy step of 1 mV. The spectrum is then integrated to yield the $I(V)$ values. These values describe the set point of experimental spectra, or the distance between tip and surface, where the feedback loop is disengaged. The results of our simulations are shown in figure 2. The onset of the surface state, its energy, and the quadratic dependence of $\mathrm{d}I/\mathrm{d}V$ on the bias is well reproduced. We note, though, that the agreement is less than perfect at the bias end-points of the simulated spectrum as compared with the experimental one. The deviation should in part be due to the high bias voltage, which will contain contributions of field emitted electrons. These contributions, expected to dominate the spectrum once the bias potential becomes comparable to the workfunction of the surface (for metals around 4–5 eV), are omitted in the simulation of the spectrum. Judging from the comparison of the experimental and simulated spectrum, contributions from the field emission regime should start to play a role at bias values of 1–1.5 V.

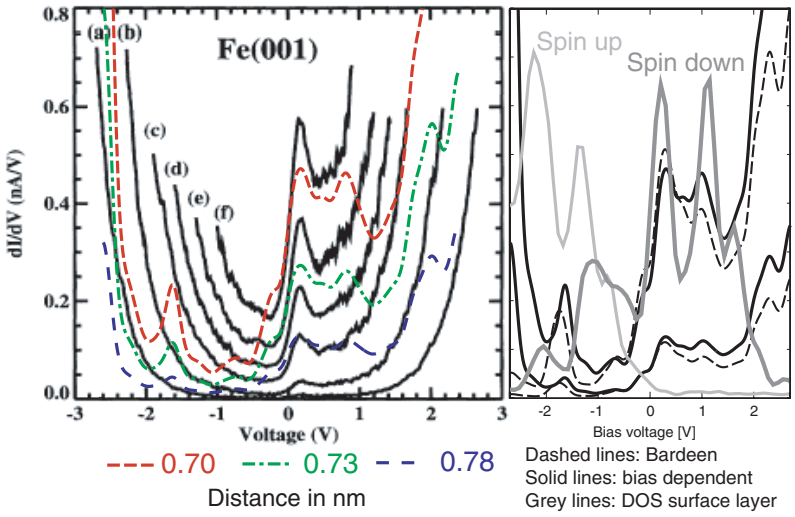

Figure 2. Left: experimental tunnelling spectrum of Fe(001) (black graphs, taken from [11]), and the spectrum simulated with an atomically sharp tungsten tip. The distance between the Fe(001) surface atoms and the tip apex is shown. The surface state yields a characteristic peak at about 200 mV; the bias dependence of the spectrum is well reproduced. Right: comparison of the Bardeen approach and the zero-order scattering approach. It can be seen that the Bardeen approach, in particular in the negative bias range, does not reproduce the bias dependence of the spectrum. For comparison we also show the density of states in the iron surface layer (grey lines): in this case neither the bias dependence nor the asymmetry of the spectrum is reproduced.

7. Summary

We have shown that tunnelling currents and interaction energies can be calculated in real space within the non-equilibrium Green function formalism based on the separate wavefunctions of the surface and tip. It was established that the zero-order expansion is equal to the traditional Bardeen approach only in the limit of zero bias and we derived the correction term for finite bias values. We also showed that successive iterations of the interface Green function with the help of Dyson's equation are feasible, since they can be reduced to products of Bardeen matrices and wavefunctions of the surface and tip. In this case higher order Green functions will lead to multiple electron pathways in the interface. These will be explored in future publications. With the help of the first-order Green function we calculated the energy of interaction between the surface and tip, and we found that it will be proportional to the tunnelling current, as stated in a previous paper [17]. Finally, we simulated the spectrum of Fe(001), measured with a tungsten tip and an iron tip over a bias range from -2.5 to $+2.5$ V. Here we find that the simulated spectrum agrees very well with experimental data, as regards the position and the onset of the surface state as well as the trends in the high bias range.

Acknowledgments

The authors acknowledge helpful discussions with A Arnau, P Echenique, M Johnson, N Lorente, J Soler, and L Wirtz. WAH also thanks the Royal Society for the award of a University Research Fellowship. KP is supported by the European Commission and the STREP project RADSAS.

References

[1] Di Ventra M and Lang N D 2002 *Phys. Rev.* B **65** 045402
[2] Meir Y and Wingreen N S 1992 *Phys. Rev. Lett.* **68** 2512
[3] Datta S 1995 *Electronic Transport in Mesoscopic Systems* (Cambridge: Cambridge University Press)
[4] Taylor J, Guo H and Wang J 2001 *Phys. Rev.* B **63** 245407
[5] Brandbyge M, Mozos J-L, Ordejon P, Taylor J and Stokbro K 2002 *Phys. Rev.* B **65** 165401
[6] Garcia-Vidal F J, Flores F and Davidson S G 2003 *Prog. Surf. Sci.* **74** 177
[7] Lorente N and Persson M 2000 *Phys. Rev. Lett.* **85** 2997
[8] Büttiker M, Imry Y, Landauer R and Pinhas S 1985 *Phys. Rev.* B **31** 6207
[9] Bardeen J 1961 *Phys. Rev. Lett.* **6** 57
[10] Hofer W A, Foster A S and Shluger A L 2003 *Rev. Mod. Phys.* **75** 1287
[11] Stroscio J A, Pierce D T, Davies A and Calotta R J 1995 *Phys. Rev. Lett.* **75** 2960
[12] Feuchtwang T E 1976 *Phys. Rev.* B **13** 517 and references therein
[13] Pendry J B, Pretre A B and Krutzen B C H 1991 *J. Phys.: Condens. Matter* **3** 4313
[14] Tersoff J and Hamann D R 1985 *Phys. Rev.* B **31** 805
[15] Chen C J 1993 *Introduction to Scanning Tunneling Microscopy* (Oxford: Oxford University Press)
[16] Lozovoi A Y, Alavi A, Kohanoff J and Lynden-Bell R M 2001 *J. Chem. Phys.* **115** 1661
[17] Hofer W A and Fisher A J 2003 *Phys. Rev. Lett.* **91** 036803
[18] Hofer W A and Garcia-Lekue A 2005 *Phys. Rev.* B **71** 085401
[19] Kresse G and Hafner J 1993 *Phys. Rev.* B **47** 558
[20] Kresse G and Furthmüller J 1996 *Phys. Rev.* B **54** 11169
[21] Blöchl P E 1994 *Phys. Rev.* B **50** 17953
[22] Perdew J P *et al* 1991 *Phys. Rev.* B **46** 6671